Systematic Identification of Preferred Orbits for Magnetospheric Missions: 1. Single Satellites.

David P. Stern
Laboratory for Extraterrestrial Physics, Goddard Space Flight Center, Greenbelt, MD 20771.

Abstract

This is a systematic attempt to identify and assess near-equatorial, high-eccentricity orbits best suited for studying the Earth's magnetosphere, in particular its most dynamic part, the plasma sheet of the magnetotail. The study was motivated by the design needs of a multi-spacecraft "constellation" mission, stressing low cost, minimal active control and economic launch strategies, and both quantitative and qualitative aspects were investigated. On one hand, by collecting hourly samples throughout the year, accurate estimates were obtained of the coverage of different regions, and of the frequency and duration of long eclipses. On the other hand, an intuitive understanding was developed of the factors which determine the merits of the mission, including long-range factors due to perturbations by the Moon, Sun and the Earth's equatorial bulge.

An overview of the Earth's Magnetosphere

The Earth's magnetosphere, the space region dominated by the Earth's magnetic field, provides a unique laboratory for studying large-scale for studying large-scale plasma phenomena of astrophysics and geophysics.

It is usually defined as a comet-shaped cavity carved in the solar wind by the Earth's magnetic field, which blocks the solar wind flow. The boundary of that cavity ("magnetopause") is rounded on the day side, where its closest distance to the Earth's center avearges 10-11 R_E (Earth radii; 1 R_E = 6371 km). It is about 15 R_E wide abreast of Earth (all distances from the center of Earth) and on the distant night side it tends to a cylinder of a radius of about 25 R_E (**Figure 1**).

Ahead of the magnetopause, in the Sun's direction, a collision-free bow shock forms, typically approaching Earth within 13-14 R_E. That shock and the "magnetosheath," the region of shocked solar wind between it and the magnetopause, are also of interest to space plasma research, especially to acceleration processes.

Many physical phenomena in and around the magnetosphere depend on the configuration of its magnetic field lines (or "lines of force"), since ions and electrons tend to spiral around such lines and thus become attached to them. Field lines on the sunward ("day") side of the Earth are compressed, while on the night side (the "tail" or "magnetotail" region) they are stretched out. The lines of the tail form two long bundles or "tail lobes". Each magnetic field line of course has a definite direction, and those of the northern tail lobe are directed **into** the region around the northern magnetic pole ("northern polar cap"), while those of the southern lobe are directed **out of** the southern polar cap, away from Earth.

Possibly the most significant region is the "plasma sheet" sandwiched between the two lobes, about 5 R_E thick. Compared to the lobes, its magnetic field is much weaker and its plasma much denser. It is the site of many active

phenomena, including impulsive "substorms" which energize ions and electrons and drive them earthward. Much of the polar aurora and of the electric currents with which they are associated comes from the plasma sheet.

The dipole-like inner magnetic field, near Earth, contains the Earth's radiation belts. The ions and electrons of the outer belt are merely the high-energy end of a much more extensive particle population named the "ring current" for the electric current which it carries, which modifies the field arising from the Earth's interior. Ring current particles typically fill the region from 3 to 9 R_E and originate in magnetic storms and substorms. The inner radiation belt, in contrast, is confin ed to a compact region near the magnetic equator (at distances of 1.3-2.5 R_E) and contains high-energy protons, a by-product of the cosmic radiation. Its magnetic effects are much weaker than those of the ring current, but it is dense enough to cause gradual radiation damage to any satellite that spends appreciable time in it, in particular to the solar cells that power such satellites.

For additional details, see *Stern and Ness [1982]* and also, on the world-wide web, *Stern [1995]*,

Missions to Study the Magnetosphere

Many unmanned spacecraft have in the past studied the Earth's magnetosphere, notably the IMP series, the ISEE, DE and AMPTE missions, and more recently Geotail, Polar, Wind, Interball, Explorer-S and Image. While most past missions have used single spacecraft or paired ones, future ones are

likely to use networks of multiple satellites, starting with "Cluster" in mid-2000.

This investigation, too, arose from the study of a "constellation" of multiple spacecraft. Named "Profile" *(Stern, [1998a, b])* that mission proposes to observe (among other things) near-radial profiles of the magnetosphere, using 12 small satellites spaced one hour apart on two slightly different orbits. This article describes what was found about the selection of single satellite orbits; a later article will focus on the multi-satellite aspects of such missions.

Space missions are inhernetly expensive and difficult. It is therefore quite important to identify orbits which give the best scientific returns. For magnetospheric missions, eccentric orbits with high apogee are often the best, because the active regions of the magnetosphere--in particular, the plasma sheet and magnetopause--lie beyond 10 R_E, while a low perigee makes data down-loading easier. The ISEE 1/2 orbits, with apogee around 23 R_E, may be viewed as typical of this class. Here we only consider low inclination orbits, best for the plasma sheet. Missions with steeply inclined orbits like those of Polar and Interball form a different class, useful for examining the region around the polar cusps, where field lines closing on the day side are separated from the ones swept into the tail.

The missions considered here tend to have multiple goals, because during the year, as Earth orbits the Sun, the axis of the spacecraft orbit, fixed in inertial space, rotates around the magnetosphere, whose axis follows the direction of the Sun and of the solar wind. If at some time the orbital axis passes the plasma

sheet, 3 months later it is directed to the flanks and 3 months after that it will be in the noon sector.

Tail Hinging and Warping

The most critical coverage in missions of the above class is that of the plasma sheet. Different choices of orbital elements lead to comparable coverage of the flanks and of the dayside (see Table 4, later on) but not of the plasma sheet. The main complicating factor is the deformation of the plasma sheet due to the varying tilt angle ψ, where $(90^0-\psi)$ is the angle between the Earth's dipole axis and a vector pointing into the flow of the solar wind, approximated by the sunward direction (**Figure 2a**).

When the Earth's magnetic axis is perpendicular to the sunward direction (as happens at times, especially near equinox), the magnetic equatorial surface, separating field lines directed away from Earth from those directed earthward, is a flat plane, identical with the magnetic equatorial plane of the Earth. For non-zero ψ, however, that surface is deformed: near Earth it follows the (inclined) magnetic equatorial plane, but past 7 R_E it gradually bends over and aligns itself with the flow of the solar wind (**Figure 2a**).

Near midnight, the effect can be approximated by following the direction of the magnetic equator up to a "hinging point" A at about $8R_E$, then continuing in the anti-solar direction (**Figure 2b**) Away from the midnight meridian the surface is further deformed by the requirement (a consequence of pressure balance) that the two tail lobes should have approximately the same cross-sectional areas. As a result, away from midnight the hinging point moves

closer to the plane OB in **Figure 2a**, and near the flanks it actually crosses that plane to its side opposite from A.

Coordinates

Described below are three relevant systems of coordinates and the notations which distinguish them here. All three are geocentric, with their origin at the center of the Earth, and in all cases the third coordinate is defined by completing a right-handed triad.

(1) Celestial coordinates (x,y,z), with z pointing northward along the Earth's rotation axis. The celestial x axis is aligned with the line of intersection between the equatorial plane of Earth and the plane of the ecliptic, in the direction of the vernal equinox, the position of the Sun around March 21.

(2) Geocentric solar-magnetospheric coordinates (x_{SM}, y_{SM}, z_{SM}), with x_{SM} pointing into the flow of the solar wind (a direction approximated by the direction to the Sun) and the (x_{SM}, z_{SM}) plane containing the Earth's magnetic (dipole) axis.

(3) Orbital coordinates (ξ,η, ζ) of the given satellite, with ζ perpendicular to the north side of the orbital plane and ξ pointing towards perigee.

The shape of the warped plasma sheet was derived using formulas obtained by *Tsyganenko [1995]*. Of particular interest here is the distance Δz from the equatorial surface, taken for an observation point given in GSM coordinates as

$\Delta z = z_{SM} - z_S(x_{SM}, y_{SM})$, where $z_S(x_{SM}, y_{SM})$ is the value of z_{SM} on the deformed equatorial surface of the point with the same (x_{SM}, y_{SM}). A FORTRAN subroutine NSHEET calculated z_S.

Metrics and Methods

Effective planning a magnetospheric mission requires the following "metrics" (quantitative measures):

(1) Criteria for evaluating a desirable orbit. These may include trade-offs that allow pne to strike a compromise between desirable and undesirable features.

(2) A list of variables whose values can be selected to determine the orbit.

(3) A method of evaluating an orbit, to decide how well it answers the mission's needs.

Using those qualitative metrics, one next seeks the optimal orbits. Two approaches exist here:

(1) Try out a large number of orbits, examine them, deduce trends which improve performance, then follow those trends until no further improvement is obtained, or until the trade-off with undesirable features is as good as can be expected. That has been the usual approach in the past.

(2) Try to develop an intuitive understanding of the factors responsible for desirable and undesirable features. Then use such understanding to limit the search to the part of parameter space where "good" orbits are expected to exist. This approach--attempted here--tries to replace purely empirical searches by systematic ones, as much as possible.

Metrics for Planning the Mission

(A) Criteria for a Desirable Orbit

(1) **Economic spacecraft**. The "Profile" mission, at least, envisioned small inexpensive satellites, lacking on-board propulsion, three-axis control or despun platforms (concerning spin, see #6 below).

(2) **Economic launch**. The thrust required to achieve an orbit with a given apogee is greatly reduced when perigee is as low as possible. At the same time, a highly elliptic orbit (apogee 20-25 R_E or more) suffers significant perturbations due to the Moon and Sun. Such perturbations keep the semi-major axis invariant, but vary the eccentricity. Orbits whose eccentricity increases are to be avoided, because perigee is then lowered and the satellite may reenter the atmosphere.

(3) Good **coverage of the plasma sheet** in the geotail. The mission may also envision observations in the near-equatorial dayside and flanks, but these (as thown in Table 4) are largely orbit-independent. This requires a low inclination to the ecliptic.

(4) **Avoidance of extended eclipses**, which can damage the spacecraft by excessive chilling. Eclipses near Earth, up to one hour, can hardly be avoided: the danger is posed by eclipses near apogee, where the satellite moves slowly and may spend up to 9-10 hours in the Earth's shadow.

Small orbital inclination to the ecliptic, which favors plasma sheet coverage (#1 above) also makes distant eclipses more likely, at a certain time of the year. Obviously, some compromise is needed.

(5) Long **orbital lifetime**. The lifetime of ISEE 1/2 was about 8.5 years, which is about as long as a mission is likely to last. Perhaps equally important, as time goes on and perturbations modify the orbit, adherence to criteria #3 and #4 above should not deteriorate.

(6) We envision a **spin-stabilized** satellite with its spin axis approximately **perpendicular** to the ecliptic. That allows plasma instruments to compare ion fluxes in opposite directions in the plane of the ecliptic. That plane is close to the equatorial surface of the plasma sheet, and from this plasma bulk motions along that surface can be deduced.

Such a spin also helps sample the solar wind when outside the magnetopause, and it assures an even input of electrical energy, at least in a cylindrical satellite surrounded by solar cells.

On the other hand, such spin all but eliminates the option of modifying the orbit by on-board propulsion, since any propulsion would have to be directed along the spin axis. This tallies with criterion #1.

(7) Avoidance of the **inner radiation belt**, which can damage the spacecraft and in particular degrade its solar cells.

That desirable feature, unfortunately, contradicts others, described earlier, and was in the end considered expendable. To avoid the inner belt, perigee would have to be raised to 3 R_E or higher, requiring extra fuel for a velocity boost of about 1.5 km/s. For a fraction of the weight of such fuel, solar cells could be protected by a 1 mm glass cover, and an extra margin of 25% in the available power could be added to compensate for their gradual degradation. The electronics and instruments can also be designed to survive the radiation, which may amount to 25 rad per pass.

Furthermore, raising perigee also makes radio communications more difficult. The greater range would require either increased transmitter power, a reduced data rate or impractically large tracking antennas.

(B) Parameters that Determine the Orbit

Given an available launch thrust, the resulting orbit is determined by the following adjustable parameters:

(a) Time of the day of the launch.

(b) Day of the year of the launch.

(c) Year of the launch

(d) Option of entering a parking orbit and delaying the

firing of the last rocket stage.

(e) Location of the launch site

(f) Direction of the initial orbit, other than eastward.

In **past studies**, only options (a)-(d) were considered. **Here** options (e) and (f) are added, and option (d) which complicates the mission was dropped.

(C) Criteria of Magnetospheric Coverage

The evaluation of orbits requires:

(a) Quantitative estimates that identify the region of the magnetosphere the satellite is most likely to be, given its location coordinates.

(b) Simulations of actual orbits, using the above criteria to estimate the time spent in each region. Such simulations can also estimate the number and duration of distant eclipses, and answer other questions.

Average boundaries of magnetospheric regions were calculated as follows. For the magnetopause we used equation (2) of *Sibeck and Roelof [1991]* , and for the location of the bow shock the equations of *Fairfield [1971]*. The equatorial surfces in the tail, depending on the tilt angle ψ, was approximated by a formula due to *Tsyganenko [1995]*. On the night side, the inner boundary of the plasma sheet was approximated by the dipole field line L=8, while the region between that and the dipole line L=6 was deemed as "transition region."

Each position (x,y,z) of the satellite's orbital simulation was converted into GSM coordinates. After that, a subroutine MSREG used the above criteria to assign the point to one of 10 regions (**Figure 2-c**), using index IREG = 0 to 9, as follows

IREG = 0	Inner magnetosphere	IREG = 5	Tail lobe
1	0-1 R_E inside magnetopause	6	Plasma sheet, $2 < \|\Delta z\| < 3$
2	0-1 R_E outside magnetopause	7	Plasma sheet, $1 < \|\Delta z\| < 2$
3	Magnetosheath	8	Plasma sheet, $\|\Delta z\| < 1$
4	Solar Wind	9	Transition region

The region around the polar cusp and above the poles was classified by IREG=10, but results are not listed here, because the orbits studied were close to the equator and never reached it.

Simulation of the Orbit

The codes used in simulating the magnetospheric coverage were developed for the "Profile" mission *(Stern, [1998a, b])* and therefore simulated not single orbits but groups of 12, differing in mean anomaly and having two slightly different values of the semi-major axis. As a result, the coverage statistics obtained here apply not to isolated missions but to ensembles of 12: this is viewed as a desirable feature, because it makes the results less sensitive to random fluctuations.

The Fortran code ORB6D3 which conducted the simulations assumed Keplerian ellipses, neglecting slow perturbations by the Moon, Sun and the equatorial

bulge of Earth. More sophisticated simulation codes, based on perturbed orbits, were also developed (naturally, they ran much more slowly). However, the output of such codes combines two separate effects on magnetospheric coverage: the choice of orbital elements, and the slow variation of those elements with time. Keplerian simulations isolate the first effect alone.

When later perturbed orbits were dealt with, their magnetospheric coverage was estimated from runs of the Keplerian code, using as inputs the osculating orbital elements given by the perturbation code for the appropriate dates. For the final choice of actual orbits, the more sophisticated codes would be used again.

All simulations covered one "short year" of 364 days (=52 weeks). Each hour of the year the position of each satellite was checked and assigned to one of the regions, and weekly coverage statistics were checked, as well as totals for the year and for each of four 13-week seasons. In addition to coverage statistics, the code also compiled eclipse statistics for locations with $x_{SM} < -2R_E$, noting each hour which satellites were shaded by the Earth and classifying eclipses by the number of consecutive hours during which a satellite was shaded. For the purpose of this calculation, the shadow of the Earth was assumed to be a cylinder, leading to a slight overestimate of the severity of eclipses.

Launch from Cape Canaveral

Most space launches by the US are conducted from Cape Canaveral, Florida, at north latitude 28.5^0. The usual launch direction is due eastward, which adds to

the launch velocity a contribution from the Earth's rotation of about 360 m/sec. If one assumes for simplicity that the spacecraft is injected into its orbit right above Cape Canaveral (rather than 1000 km or more to the east, where orbital velocity is finally achieved), then the initial perigee will also be above Cape Canaveral, and therefore the orbital inclination i to the Earth's equator will be 28.5^0.

The radial line to the perigee point will lie on a cone around the Earth's axis, with opening angle 61.5^0 equal to the co-latitude of Cape Canaveral (**Figure 3**), Because of the inclination angle $\varepsilon = 23.5^0$ between the Earth's axis and the z_e direction perpendicular to the ecliptic, the orbital inclination i_e to the ecliptic on any launch date can be anywhere from $(28.5-23.5) = 5^0$ to $(28.5+23.5) = 52^0$, depending on the time of the day when the launch occurs. On any day, we define as the *reference time* the time when a launch gives i_e its minimum value. For an orbit launched at such a time, the argument of perigee is $\omega = 90^0$ and the longitude of the ascending node is $\Omega = 0$.

Unfortunately, such a launch leads to a very poor phasing between the orbit and the hinging of the midnight plasma sheet. Since perigee is then 5^0 north of the ecliptic, apogee will be south of it. However, as Figure 3 shows, this choice of launch places apogee in the tail at the summer solstice when the axial tilt ε of the Earth's axis gives the midnight equatorial plane its greatest northward displacement.

The average tilt angle ψ at solstice also equals ε, modulated in a diurnal cycle by about 50% because of the 11^0 angle between the Earth's magnetic axis and its rotation axis. Because of the hinging effect, the midnight plasma sheet will

also be near its greatest northward displacement, while the satellite at its apogee (where much of the mission's time is spent) is south of the ecliptic and is likely to miss it altogether.

Parking Orbits

One way of avoiding this problem is to first launch the spacecraft into a circular parking orbit, and then after a suitable interval fire the last rocket stage into the final elliptical orbit. The circular orbit determines the orbital plane, but not the value of ω, which on that plane gives the direction of the perigee point. By choosing the time when the last stage is fired, ω can be given any value from 0^0 to 360^0. Allowing the spacecraft to traverse an angle δ in its parking orbit yields $\omega = 90^0 + \delta$, so that by delaying the firing of the last stage by 1/4 orbit (or by (2N+1)/4 orbits, with N some integer) the line of apsides is rotated by 90^0, from the plane of Figure 3 to a direction perpendicular to that plane, parallel to the celestial x-axis. We will call this the "reference orbit."

The reference orbit provides very good coverage of the plasma sheet. However, by placing apogee in the plane of the ecliptic, it practically assures long eclipses around the time of equinox. To prevent this from happening, the orbit must be "detuned" from the reference orbit in one of two ways: either by making δ larger or smaller than 90^0, or by advancing or delaying the launch by a few hours, relative to the reference time.

Table 1a

Delay → / Coast angle ↓	−2	−1	0	1	2	3 hours
50⁰	6 (31)	8 (41)	5 (12)	2 (83)	2 (14)	1 (248)
60⁰	5 (12)	7 (21)	6 (10)	2 (98)	2 (12)	1 (248)
70⁰	4(6) 3(54)	6(4) 5(40)	7 (22)	2 (122)	2 (24)	1 (246)
80⁰	3 (23)	4 (41)	8 (24)	3 (15)	2 (52)	2 (36)
90⁰	2 (82)	3 (66)	9 (12)	3 (59)	2 (96)	2 (66)
100⁰	2 (54)	3 (30)	8 (31)	4 (35)	3 (23)	3 (12)
110⁰	2 (30)	2 (117)	7 (28)	6(3) 5(35)	4 (16)	3 (42)
120⁰	2 (12)	2 (111)	6 (14)	7 (23)	5(8) 4(45)	4 (31)
130⁰	2 (17)	2 (74)	5 (19)	9(1)8(29)	7(3)6(40)	6 (18)
140⁰	2 (30)		4 (32)		8 (30)	8 (12)

Table 1b

Delay → / Coast angle ↓	−2	−1	0	1	2	3 hours
50⁰	7623	5187	4263	3388	3087	2380
60⁰	9275	7301	5551	4473	3549	2954
70⁰	8526	7504	6272	5719	4319	3514
80⁰	7287	7357	6524	6643	5425	4165
90⁰	6447	7056	6370	6993	6300	5054
100⁰	5418	6503	6223	7257	7084	5915
110⁰	4242	5663	6181	7399	8239	7210
120⁰	3535	4347	5474	6930	8925	8876
130⁰	3052	3304	4172	4970	7287	8603
140⁰	2408		3143		5019	6706

Detuned Orbits

Any such "detuning" implies a compromise: the duration of eclipses should be reduced to tolerable limits, while the coverage of the plasma sheet should not suffer too badly. Tables 1a and 1b give the results for a 67 hour orbit (more precisely, for an ensemble of six 66-hour orbits and six 68-hour ones), corresponding to an apogee near 25 R_E (perigee is 1.1 R_E). Table 1a counts the hours spent (by any one of the 12 satellites) during the year in the plasma sheet within 1 R_E of the equatorial surface--i.e. with IREG = 8; times with IREG=6 and IREG=7 are comparable. In a short year of 52 weeks, a dozen satellites total 104,832 hours of observation, so as a rough rule, each 1000 hours recorded on that table ar equal to about 1% of the observing time. Note that the best coverags is obtained not with the reference orbit but with orbits delayed by 2-3 hours from the "reference time", and with $\delta = 120^0$.

Table 1b tallies distant eclipses in the same orbits; each cell gives the length in hours of the longest eclipse, and the number of such eclipses recorded for 12 orbits. A few of the entries also include (in parentheses) eclipses one hour shorter than the maximum, in general much more numerous, and those shorter by two hours are more numerous still. All there tallies must be divided by 12 to give the average per satellite.

Comparing the two tables shows that orbits with the best plasma sheet coverage also have the longer eclipses. There exist no bargains, only some reasonable compromises. A delay of 2 hours and $\delta = 60^0$ places the satellites in the central plasma sheet about 3.5% of the mission (or about 10% within 3 R_E of

the equatorial surface) at the price of one 2-hour eclipse per year. If the mission can annually afford two 3-hour eclipses (and a fair number of 2-hour ones), $\delta = 100^0$ gives about twicethe above plasma sheet exposure.

Table 2a

Delay → / Coast angle ↓	−2	−1	0	1	2	3 hours
50^0	6 (4)	7 (1)	5 (1)	2 (136)	2 (23)	1 (354)
60^0	4 (71)	6 (13)	5 (58)	2 (132)	2 (12)	1 (356)
70^0	3(97)	5 (31)	6 (35)	2 (167)	2 (36)	2 (3)
80^0	3 (22)	4 (30)	7 (11)	3 (25)	2 (72)	2 (36)
90^0	2 (128)	3 (68)	7 (22)	3 (84)	2 (122)	2 (93)
100^0	2 (75)	3 (24)	7 (9)	4 (16)	3 (20)	2 (136)
110^0	2 (41)	2 (168)	6 (36)	5(34)	3 (71)	3 (39)
120^0	2 (18)	2 (138)	5 (47)	6 (12)	4 (46)	4 (24)
130^0	2 (22)	2 (128)	4 (87)	7(10)	6 (6)	5 (25)
140^0	2 (36)	2(124)	4 (5)	7(4)	7 (6)	6 (43)

Table 2b

Same as table 1b, but for orbital periods 47±1 hours.

Delay →	−2	−1	0	1	2	3 hours
i_e	13.9⁰	8.25	5.05	8.25	13.9	19.86
ω_e	-124.1	-134.1	−180.	134.1	124.132	124.091
Ω_e	−82.98	−59.37	0.	59.37	82.98	96.79
↓ Coast angle						
50⁰	7672	6069	4900	4550	4060	3185
60⁰	10255	7777	6216	5229	4606	3878
70⁰	10514	9163	7532	6797	5376	4557
80⁰	9296	9114	8190	7994	6902	5670
90⁰	8414	9058	8477	9233	8554	7574
100⁰	7399	8505	8589	9912	10395	9541
110⁰	6006	7196	8099	9632	10892	11053
120⁰	4585	5600	6202	8050	9590	10682
130⁰	3297	4081	4424	5243	4613	8750
140⁰	2835	2835	3346	3654		5824

Of course, any fit tuned so finely is not likely to persist to the next year's apogee pass through the tail, because of orbital perturbations due to the Moon, Sun and the equatorial bulge of the Earth. Tables 2 give corresponding numbers for orbits of 47±1 hours, with apogee around 20 R_E. Plasma sheet coverage is typically 30% higher, but these orbits miss the interesting region around 25 R_E where (according to many claims) magnetic reconnection in substorms begins.

Launches from points near the Equator

Adding to the mission a parking orbit and delaying the firing of the last stage requires 3-axis control (the rocket needs to be rotated) and adds complexity, increasing the risks. In addition, the final orbit is just a compromise, balancing plasma sheet coverage against distant eclipses. Fortunately, an alternative exists, providing good plasma sheet coverage without the penalty of long eclipses--namely, by launching from a site near the equator.

Such launches may be carried out either from the launch site of the European Space Agency (ESA) in Kourou, French Guiana (lat. 5^0N, long. 52.5^0 W), or from the recently introduced "Sealaunch" ship *[Smith 1999a, b]* , as well as with the "Pegasus" rocket launched from a B-52 airplane. The arguments developed earlier for Canaveral launches show that such sites can readily provide orbits with zero inclination i_e to the ecliptic. If apogee is then at midnight during equinox (which would require a parking orbit), satellites would be in the plasma sheet essentially all the time they spent on the night side. That would give the greatest possible coverage, but distant eclipses would also be frequent, and they would have the longest possible duration, up to 9-10 hours with 25 R_E apogee.

What is proposed here is quite different, and assumes launches timed near the "reference time" defined earlier. For orbits launched from Kourou, this would produce an inclination to the ecliptic of $i_e = 5-23.5 = -18.5^0$, i.e. perigee will be south of the ecliptic (this corresponds to $i_e = 18.5^0$, with ω and Ω shifted by 180^0). Because i_e is now large, few eclipses are expected in the distant part of the orbit, near apogee.

As shown earlier, orbits launched at the "reference time" (with no delay in a parking orbit) place apogee in the tail during summer solstice, when the midnight plasma sheet is shifted as far north as it can go. Unlike the orbit launched from Cape Canaveral, however, this one has perigee south of the ecliptic, and its apogee therefore is also north of the ecliptic. That produces in the summertime a substantial overlap between the orbit and the plasma sheet (**Figure 4**). In other words, this orbit takes advantage of the plasma sheet's warping to obtain both good coverage and reduced eclipses.

Table 3 compares a number of near-equatorial launches, each calculation combining 12 orbits with periods 67±1 hours, i.e. with apogee near 25 R_E. All launches are either at the reference time or with delays of up to several hours, as noted. The assumed longitude is always that of Kourou (-52.5^0), but the latitude is either that of Kourou (5^0) or as indicated on the table. Two orbits from Cape Canaveral are included for comparison, one of them (#3, marked *) using a parking orbit and delayed firing.

For each mission, the table lists the annual number of hours spent in regions 6, 7 and 8 of the plasma sheet, the length in hours of the longest eclipse and the annual number of such eclipses for 12 orbits--and in parentheses, the same information for the second-longest eclipse. The following features are illustrated by the table:

(1) Runs #1 and #2 compare two missions from Kourou with the same orbit, except that in #2 the starting positions of all satellites are shifted ahead by 20 hours. That gives a simulation which is equivalent but not identical, and the difference helps one estimate the random variations

expected between members of an ensemble of equivalent orbits. A variation is evident, but it is small. Note that the longest recorded duration of a distant eclipse is just one hour.

(2) Runs #3 and #4 are comparison orbits from Cape Canaveral, with (#3) and without (#4) a delay in a parking orbit. Run #3 (marked *) is the "optimally detuned" orbit described in an earlier section. Note that the plasma sheet coverage of run #4 is quite poor, due to the fact (also noted in **figure 3**) that on this orbit, when the satellite is in the tail, it is south of the ecliptic, while the midnight plasma sheet has its greatest displacement north of the ecliptic.

Table 3

Run	lat	delay hours	IREG=6	IREG=7	IREG=8	longest eclipses	number
1	5	0	6755	5824	6090	1 hour	258
2	5	0	6650	5880	6020	1	114
3	28.5	2*	5670	3808	3528	2	9
4	28.5	0	4578	756	56	2	217
5	5	1	7182	6076	6195	2 (1)	24 (243)
6	5	2	7679	6706	6944	2 (1)	78 (126)
7	5	3	7441	7427	8197	3 (2)	57 (65)
8	5	4	6916	7854	8827	5 (4)	26 (24)
9	5	-1	7308	6027	6342	2 (1)	24 (243)

1	5	0	6783	5873	6027	1	252
10	10	0	7609	8995	9527	2 (1)	24 (300)
11	15	0	7448	10227	11662	2 (1)	76 (331)
12	20	0	7210	6307	8470	3 (2)	113 (216)

11	15	0	7448	10227	11662	2 (1)	76 (331)
13	15	1	7049	9821	11522	3 (2)	18 (108)
14	15	-1	7035	9891	11389	3 (2)	12 (108)
10	10	0	7609	8995	9527	2 (1)	24 (300)
15	10	1	7784	8701	9954	2 (1)	60 (258)

Table 4

IREG =	0	1	2	3	4	5	6	7	8	9
#1	11179	5411	4998	17955	31199	14581	6755	5824	6090	560
#2	11172	5418	4991	17934	31185	14679	6650	5880	6020	609
#3	9961	5292	4893	17381	31920	21175	5670	3808	3528	574
#4	9534	5117	4865	17136	31640	29309	4578	756	56	504

Table 4 gives the annual number of hours spent in each region of the magnetosphere (total for 12 satellites), for runs #1 to #4 of Table 3. It is evident that the choice of orbit can make a great difference in the way

magnetospheric coverage on the nightside is divided between the plasma sheet and the tail lobes, but that coverage of other regions is largely unaffected.

(3) Runs #5-9 refer to launches from Kourou, at times shifted by −1 to 4 hours from the reference time. Note that coverage is slightly improved, but at the cost of 2-hour eclipses for shifts of 1-2 hours and even longer ones for greater shifts.

(4) Runs #10-12 (with run #1 added for comparison) give the effect of increasing the launch latitude in steps of 5^0. It is evident that launching from 10^0 gives much better covereage, and 15^0 is even better. The reason is that the ecliptic inclination of $i_e = 18.5^0$, obtained with Kourou, is steeper than the optimum: as Figure 4 shows, the orbit crosses the equatorial surface and apogee is likely to be too far north of it. Unfortunately, eclipse length also increases, because each 5^0 increase in latitude (for launches at the reference time) also decreases i_e by 5^0, and orbits with small i_e are much more susceptible to distant eclipses. Still, launch from latitude $10\text{-}12^0$ may turn out to be the optimal choice.

(5) Finally, runs #13-15 (with #10 and #11 repeated for comparison) give results for launches from latitudes $10\text{-}15^0$, delayed or advanced by one hour. No clear advantage in coverage is seen, and eclipses are somewhat longer.

The final conclusion seems to be that orbits launched at the "reference time" from latitudes 5^0 or 10^0, whose apogee is at midnight around the (northern) summer solstice, give about twice the plasma sheet coverage as "optimally

detuned" orbits from Cape Canaveral which use a parking orbit and delayed last stage firing. Eclipse exposures are comparable or shorter.

Orbital Perturbations

A low perigee orbit extending to 20-25 R_E undergoes marked perturbations by the gravitational attractions of the Moon, Sun and the Earth's equatorial bulge. However, since perigee altitudes of all acceptable orbits were above 600 km, air resistance was neglected. On a scale of years and decades, the osculating semi-major axis a does not undergo any significant changes. However, the orbital eccentricity e may vary, raising or lowering the radial distance R_P of the perigee point. To achieve the most economical launch one would prefer to start with the lowest possible R_P (requiring the smallest injection velocity) but under conditions where R_P grows with time.

Over the long range, R_P both rise and falls, and sooner or later (for the orbits considered, typically within a decade or two) those variations cause the satellite to re-enter the atmosphere. This may be a desirable feature, ensuring that the mission does not contribute to long-term space debris. Perturbations will also change other orbital elements, so that orbits carefully chosen for high plasma sheet coverage and short eclipses are likely to lose their advantage in later years. This type of deterioration, as it turns out, may well be the most significant factor limiting the duration of missions.

The ENCKE2 Code

The perturbed orbit was derived by numerical integration using Encke's method *(e.g. Danby [1988]; Battin [1964])*. This method works well with periodic orbits which at any time approximate Keplerian ellipses with slowly varying "osculating" orbital elements. Most orbital calculations nowadays use all-purpose commercial codes (e.g. "Satellite Toolkit" or STK) based on straight-forward integration of Newton's laws, relying on powerful computing machines. Encke's method is however still used occasionally, e.g. in the "Grave" code by Roger Burrows, used by *Mullins and Evans [1996]* for calculating proposed orbits for the AXAF mission (now operational under its new name, Chandra). The ENCKE2 code (developed by the author) allowed great flexibility, including the calculation of many satellite positions throughout the year.

The idea behind Encke's method is straightforward. At the initial location P of the satellite, the local orbit is approximated by an "osculating" Keplerian motion, derived from the spacecraft's current position and velocity without taking any perturbations into account. At subsequent times, the calculation follows this osculating orbit and at each point calculates the correction to the satellite's position and velocity due to the perturbing effect of the Moon, Sun and bulge. This is not absolutely accurate, because the correction is calculated not at the point reached by the actual motion, but at the corresponding point on the osculating ellipse. Still, as long as the two are not far apart, the error introduced in this manner is very small.

When the difference between the osculating orbit and the actual one exceeds a certain limit (chosen by the user and depending on the accuracy desired), the orbit is "rectified" and the previously used osculating elements are

replaced with the current ones, including the accumulated effect of the corrections to the motion. The output of the code is thus a collection of sets of orbital elements, each labeled by the time at which it supersedes the previous set. With ENCKE2 rectifications were typically performed about one day apart.

The outputs of the code were compared to those of *Mullen and Evans [1996]* and to orbits derived in 1997 by Stacey Prescott and Brian Sinclair of the US Naval Academy, using the Satellite Toolkit. They matched in all details, except (as noted below) in the predicted behavior of the AXAF semi-major axis.

A detailed discussion of the perturbation code is obviously beyond the scope of this article. However, three points in which this code may differ deserve to be mentioned:

(1) Several choices of integration algorithms were tried, all based on the Runge-Kutta approach as described by *Press et al. [1992]* . The long-term constancy of the semi-major axis a (expected from general theoretical principles) was taken as a sensitive criterion for the accuracy of these algorithms. With regular Runge-Kutta methods, the value of a tended to slowly drift

This drift was eliminated by the algorithm of Bulirsch and Stoer, also given by *Press et al. [1992].* That algorithm starts with a relatively crude variant of the Runge-Kutta integration, then subdivides the integration interval h and repeats the calculation, subdivides again with still smaller h and repeats again, until a number of such approximations is obtained, each with its step-size h. If one could use an arbitrarily small

value of h, the result could be made arbitrarily accurate--but in practice, of course, one cannot go that far. However, one can fit the results obtained with different values of h to a polynomial (a polynomial in h^2 may be shown to suffice), and the results are then extrapolated to $h=0$. The limiting value obtained in this manner is surprisingly accurate.

Bulirsch-Stoer integrations of the orbit produced a steady unvarying value of the semi-major axis a (**Figure 5a**). In contrast, *Mullen and Evans [1996]* used Runge-Kutta integration and as shown in their figure (3a), in the course of 50 years their value of a slowly drifted. ENCKE2 repeated that calculation and found no drift, while completely matching their figures (3b) and (3c), suggesting that the drift in a did not invalidate their other results.

(2) As noted, three sources of perturbation were taken into account--Moon, Sun and the bulge of the Earth. The effects of the first two do not follow any simple pattern, but those of the bulge need to be handled with care.

Suppose the bulge were the only source of perturbation. Even with that perturbation, the gravity field is still axisymmetric, and therefore the orbit has a constant shape, in a plane which usually rotates slowly around the Earth's axis. Far from Earth, the perturbation is small and the field is well approximated by a gravitational monopole, so that one expect that part of the orbit to closely resemble a Keplerian ellipse. Near Earth, however, it would significantly differ from an ellipse.

Thus, if one uses the local position and radius at any instant to calculate the osculating ellipse (as was done here), the result will depend on the part of the orbit where the derivation was performed. Derivations far from Earth would yield very nearly the same osculating elements, e.g. the same semi-major axis a ; but points near perigee would give significantly different values. That systematic variation persists when perturbations due to the Moon and the Sun are added.

If orbital rectifications are performed whenever the appropriate criterion is satisfied, they will be randomly distributed around the orbit. Some will happen near perigee, and the new osculating elements which they would yield would be quite inappropriate for most of the orbit, adding to the "random noise" in the output. A simple and effective remedy, practiced here, was to postpone any rectifications that were scheduled within a time T of a perigee pass, with T typically equaling 2 hours.

(3) In calculating the perturbations due to the Sun and the Moon, their positions need to be calculated for every point of the orbit. We used for this "low precision formulas" from the US nautical almanac, which give the Moon's position within 0.2 R_E, while other celestial motions and times were derived using formulas by *Meeus [1991]*. These derivations can appreciably slow down the calculation--especially for the Moon, where even the simplified formulas involve 40 terms and 16 trigonometric functions. For both bodies, calculation time was greatly reduced by only deriving the positions of the Sun and the Moon every 12 hours, and interpolating in-between.

One caution must however be observed. Let A and B in **Figure 5b** be two positions of the Moon between which interpolation is performed, while O is the center of the Earth. If the interpolation is linear, since AB is a chord of the Moon's orbit, any interpolated point will always be closer to the Earth's center than the corresponding point on the actual orbit.

To avoid a systematic error from this cause, the actual interpolation was performed not between A and B but between A' and B', where the area of the triangle A'B'O equaled that of the orbital segment ABO, here approximated by a section of a circle. Stated in different terms, any linear interpolation between orbital points such as A and B is equivalent to approximating the orbital curve by a polygon. Here, instead of using an inscribed polygon, which will always be smaller than the actual orbit, we used a polygon of similar shape, but magnified by a factor f slightly larger than 1, giving it the same area as the actual orbit. All interpolated coordinates are then also multiplied by that factor f. That was the procedure adopted for the Moon: with the Sun, the angle AOB was so small that no such correction was held necessary.

Launch Timing and Orbital Perturbations

The bottom curve in **Figure 6** shows the predicted 10-year behavior of the radial perigee distance R_P for a typical orbit, in this case with a period of 67 hours (apogee near 25 R_E), launched due east from a site on the equator, longitude 40 W and with initial value $R_P = 1.1\ R_E$. **Figure 7** gives a magnified view of the first 1.5 years of that curve.

It is evident that perigee height undergoes three types of change: a semi-monthly wave of about 100 km peak-to-peak (PTP), a semi-annual one of about 850 km PTP, and a long scale irregular variation. All these changes reflect corresponding changes in the orbital eccentricity *e*. With a 20-R_E apogee similar changes were observed, but their amplitude was reduced, so that the semi-annual wave was only about 600 km PTP.

Experimentation with orbits has shown that these curves are fairly robust: for instance, raising the initial perigee by 1000 km or by 2000 km yielded a very similar variation of the perigee height, but with all points lifted by about 1000 km (as in the higher curves of **Figure 6**). Thus given a satellite orbit, starting with a given velocity from a predetermined perigee distance(e.g. from 7000 km, close to 1.1 R_E), its subsequent perigee distances will depend on the phase of the launch date in the semi-annual perigee cycle.

If launch occurs at the peak of the cycle, perigee height on subsequent orbits will steeply decrease, and since the bottom of the curve is around 6150 km, while the dense atmosphere starts around 6500 km, the satellite is almost certain to be lost. On the other hand, if launch is timed to be near the semi-annual minimum, the perigee height of later orbits will rise, and in the absence of other variations, it will not fall significantly below 7000 km.

Thus the first step in planning long-term missions is a fairly simple one. Using an orbital code, derive an orbit similar to the one being planned, starting slightly before the earliest acceptable launch date. Then plan the actual launch time around one of the minima of the semi-annual wave of

perigee distance which you have obtained. This would give two fairly broad launch windows per year, half a year apart. For even greater economy, one might launch around one of these minima at a time when the semi-monthly wave also hits minimum (see Figure 7). That can add nearly 100 km to the perigee altitude, but the launch window now shrinks to a day or two.

In addition to the two periodic variations, a long-term trend also exists. In the example shown, perigee rises for two years, drops back over two years and then continues with milder changes. Some orbits display only minor changes, while others, like the one calculated by *Mullen and Evans [1996]* change quite dramatically. In particular, orbits near the critical inclination of $i = 63.4^0$ (arc sin $2/5^{1/2}$) may evolve quite rapidly. For instance, the perigee of Russia's Interball-Tail satellite *[Galeev et al., 1996],* launched 3 August 1995 with $i = 62.9^0$, rose during the first year of the mission from its initial value of 7172 km to nearly 3 R_E. Of course, such steeply inclined orbits slice through the plasma sheet almost perpendicularly, and spend relatively little time there.

Long-term trends also exhibit a certain amount of robustness, though one may have to experiment with several close orbits to see which fits best. The timing of the launch studied in Figures 6--July 1, 2000--is well-chosen, at the start of a rising trend. Launch in 2003, on the other hand, may encounter a trend of declining perigee, causing early loss, while the middle of 2005 is again at the bottom of a rising trend, albeit a milder one.

The variations of the inclination, the argument ω of perigee and the longitude Ω of the ascending node, for the above orbit, are given in **Figures 8a - 8c**.

Eclipses and the angle χ

Eclipses are the bane of orbits with moderate inclinations to the ecliptic--an unfortunate thing, because these are also the orbits with the best plasma sheet coverage. Such coverage becomes even more important when one deals with a cluster or constellation of satellites, when it is not only important for the satellites to cover that region, but to do so concurrently.

The effect on distant eclipses due to variations of the conventional orbital elements (i, ω, Ω) is not easy to interpret intuitively, since a mixture of factors is involved. A much more intuitively significant parameter is the angle χ between the line of apsides--the long axis of the orbital ellipse--and the plane of the ecliptic; that is, $(90\text{-}\chi)$ is the angle between that line and the ecliptic z-axis, perpendicular to the plane. With χ less than 10^0 distant eclipses are likely, and when χ is close to zero they are at their maximum duration. Reducing the inclination i_e to the ecliptic also tends to prolong distant eclipses, but χ is the main factor.

The strategies developed with Keplerian codes, seeking the fewest and shortest eclipses, practically assure that at the start of the mission χ is large. Unfortunately, after performing many orbital simulations, it was found that χ inevitably oscillates around $\chi=0$, with a typical period between 5 and 15 years (**Figure 9** gives an example). Thus if we start at the peak of the cycle, χ will decrease and will typically pass $\chi=0$ within about 2-3 years.

One could hope to improve the situation by "detuning" the orbit slightly, but that does not work out. The "reference orbit" has $\Omega=0$. If one starts instead

from $\Omega>0$, the initial value of χ is already past its extremum and therefore reaches $\chi=0$ even sooner than before. Starting with $\Omega<0$ gives an initial value of χ preceding the extremum, so that more than a quarter-oscillation elapses before $\chi=0$ is reached; however, the wavelength of the oscillation is reduced, so that the total time elapsed from launch to the crossing of $\chi=0$ stays about the same. Starting from latitude 10^0 instead of 5^0 will reduce the amplitude of those oscillations (reducing the average of χ and therefore increasing eclipse durations) but does not change their period.

In practice this seems to say that only the first year's passes through the tail will avoid long eclipses. A long term mission of this type is still feasible, but only if the spacecraft can survive intense chilling. Because the DOY (day of year) of midnight passage changes only slowly (top curve in Figure 9) the coverage of the plasma sheet is not expected to deteriorate too much.

Fine-tuning the time of $\chi = 0$

A method was developed for moderating the effect of the passage through $\chi=0$, but unfortunately the advantage gained by it is relatively slight.

Experimentation with orbits has shown that if the launch is delayed by half a year, the curve of χ against time t remains very similar, except that it is shifted ahead by half a year. Previously it was found that (for a given orbit) each year has two launch windows half a year apart, at the minima of the semi-annual variation in perigee height. They allow one to choose between two different times when $\chi=0$, about half a year apart.

By launching from a site like Kourou at the "reference time" of the day, one assures that the satellite is in the tail around the summer solstice. (By the way, by launching from a site south of the equator about 12 hours off the reference time, one obtains a "mirror image" orbit which passes the tail around the winter solstice, reaping similar benefits.) Of the two launch windows, it is therefore preferable to choose the one which makes $\chi=0$ occur in winter, when perigee is on the day side.

The time when $\chi=0$ can be shifted somewhat by launching not due east, but at some small angle γ to the easterly direction, which increases the inclination i to the Earth's equator. For small values of γ, typically, every 5^0 in γ shifts the time of $\chi=0$ by 2 months, which may be sufficient to place that time near the winter solstice. Of course, orbits not launched in the easterly direction do not reap the full benefit of the Earth's rotation (360 m/s at Cape Canaveral, 407 m/s on the equator), but the penalty Δv is rather small:

γ	Δv
5^0	1.548 m/s
10^0	6.183 m/s
15^0	13.868 m/s
20^0	24.55 m/s

The bad news is that the variation of χ near the $\chi=0$ time is not fast enough to avoid substantial eclipses. If $\chi=0$ occurs at the winter solstice, apogee passes midnight half a year before and after, at which time $\chi=2^0$ and eclipses are still 6 hours long (whereas at $\chi=0$ they reach 9-10 hours).

Summary

A systematic procedure was developed to identify, evaluate and study orbits of scientific satellites that study the Earth's magnetosphere, in particular its plasma sheet and magnetotail. All these missions involve highly eccentric near-equatorial orbits, with initial perigee distances around 1.1 R_E and typical apogee distances of 20-25 R_E.

The selection and study of such orbits proceeds in three steps:

(1) Establish quantitative criteria or "metrics" by which the suitability of different missions may be compared. Such metrics also include all factors whose values determine the initial orbit

(2) Study the full range of available Keplerian orbits, to see which range of orbital elements best meets the criteria of #1.

(3) Simulate and study the evolution of the selected missions in subsequent years, due to gravitational perturbations by the Moon, Sun and the equatorial bulge of the Earth. Use such studies to improve strategies for selecting the mission.

In step #1, three types of metrics were particularly important:

(a) The mission should use inexpensive small spinning satellites, with their spin axis approximately perpendicular to the ecliptic. The orbits should require a minimal boost, achieve good coverage of the plasma sheet and of other interesting regions, have long lifetimes and avoid lengthy eclipses.

(b) The factors which affect the initial orbits are time of day of the launch, day of the year, and the year of launch itself. An option of launching into a parking orbit and then delaying the firing of the last stage was also studied, as was the option of launching from sites other than Cape Canaveral and into directions other than due east.

(c) To evaluate coverage of various magnetospheric regions, subroutines were created which, given a point in space and some time, named the magnetospheric region in which the point was most likely located. Keplerian codes were then produced which tracked satellites hour by hour throughout the year, collecting statistics on region occupancy, eclipses and their durations, and other information.

Step #2

An important parameter in determining both coverage of the plasma sheet and eclipses was the orbital inclination i_e to the ecliptic. A second factor was the time of the year in which apogee was at midnight, which because of the warping and hinging of the plasma sheet, greatly affected plasma sheet coverage. Using the Keplerian simulation described above, many such orbits were studied and their statistics were compiled and compared.

For launches from Cape Canaveral, the best orbits were obtained by sending the spacecraft into a parking orbit with moderately small i_e and then waiting about a quarter of an orbit before firing the last stage, needed to achieve the final apogee. This method requires accurate 3-axis control in the parking orbit and was judged to be somewhat risky.

Orbits of much better quality--shorter eclipses, nearly twice the plasma sheet coverage and no need for a parking orbit--were obtained by shifting the launch site to latitudes 5 - 10^0, choosing a relatively steep i_e and placing apogee in the tail at a time when its deformation, due to the tile of the Earth's magnetic axis, was at its maximum.

Step #3

In the long-term evolution of an orbit, it is important to avoid early atmospheric re-entry and long eclipses. One would furthermore like to preserve good plasma sheet coverage, but that in any case only changes slowly.

Early re-entry is avoided by launching at one of the semi-annual minima of the perigee distance, whose location can be establishing by examining a similar orbit starting a year or so earlier. A fairly long lifetimes may be achieved by examining the long-term trend of the perigee height (again, using a similar orbit for guidance) and timing the launch to coincide with a gradual rising trend in perigee height.

Avoiding distant eclipses is much more difficult. They depend most strongly on the angle χ between the ecliptic and the long axis of the orbital ellipse, and are worst near $\chi = 0$. Unfortunately, on all orbits tested χ tends to oscillate with periods of 5-15 years, so that even if initially χ is close to its peak value, within 1/4 of a period, $\chi=0$ is crossed, producing long eclipses. One can ameliorate this problem by having $\chi=0$ occur when apogee is near noon, but even then, half a year before and after that time χ is small enough to create problems.

Many of these problems are avoided by increasing i_e, but then coverage of the tail is also greatly reduced, which is particularly unfortunate in a "constellation" mission of several spacecraft. The problem could also be solved by technology, if satellites could be designed that can endure the severe chilling of a 7-hour eclipse. For this one might even consider battery-free satellites which shut down completely in the Earth's shadow and "re-awaken" afterwards.

References

Battin, Richard H., *Astronautical Guidance*, xiv + 400 pp., McGraw Hill, New York, 1964.

Danby, John M.A., *Fundamentals of Celestial Mechanics*, 2nd edition, corrected and enlarged, xii + 483 pp., Willmann-Bell, Inc., Richmond, VA, 1992.

Fairfield, Donald H., Average and unusual locations of the Earth's magnetopause and bow shock, *J. Geophys. Res., 76*, 6700-6716, 1971

Galeev, A.A., Yu. I. Galperin and L.M. Zelenyi, The Interball Project to study Solar Terrestrial Physics, *Kosmicheskiye Issledovania , 34*, 339-62, 1996, English translation *Cosmic Research, 34*, 314-333, 1996.

Meeus, Jean, *Astronomical Algorithms*, iv + 429 pp, Willmann-Bell, Richmond, VA 1991.

Mullins, L.D. and S. W. Evans, The dynamics of the proposed orbit for the AXAF satellite, J. Astronaut. Sci., 44, 39-62, 1996

Press, William H., Saul A. Teukolsky, William T. Vetterling and Brian P. Flannery, *Numerical Recipes,*, 2nd ed., xxvi + 963 pp., Cambridge U. Press., 1992.

Sibeck, D.G., R.E. Lopez and E.C. Roelof, Solar wind control of the magnetopause shape, location and motion, *J. Geophys. Res., 96,* , 5489-95, 1991.

Smith, Bruce, Sea Launch Mission to Demonstrate System, *Aviation Week & Space Technology*, p. 74-78, March 22, 1999a

Smith, Bruce, Sea Launch Passes Demonstration, *Aviation Week & Space Technology*, p. 65, April 5, 1999b

Stern, David P., Planning the "Profile" Multiprobe Mission, p. 136-141 in *Science Closure and Enabling T echnologies for Constellation Calss Missions,* V. Angelopoulos and P. V. Panetta, eds., Berkeley Univ., 1998a. [Also: http://www-istp.gsfc.nasa.gov/profile/Monogr1.htm]

Stern, David P., Science tasks for "Profile", p. p. 66-71 in *Science Closure and Enabling T echnologies for Constellation Calss Missions,* V. Angelopoulos and P. V. Panetta, eds., Berkeley Univ., 1998a. [Also: http://www-istp.gsfc.nasa.gov/profile/Monogr2.htm]

Tsyganenko, N.A., Modeling the Earth's magnetospheric magnetic field confined within a realistic magnetopause, *J. Geophys. Res., 100,* 5599-5612, 1995.

Captions of Figures

(1) Schematic view of the Earth's Magnetosphere

(2a) The hinging of the midnight plasma sheet, due to the tilt angle ψ of the Earth's dipole axis

(2b) The warping of the plasma sheet away from the midnight meridian.

(2c) The classification of magnetospheric regions used in this study.

(3) The variation of the orbital inclination i_e of orbits launched from Cape Canaveral (lat. 28.5^0N), varying from 5^0 to 52^0 depending on the time of day on which the launch took place. The time when i_e is minimal will be called the "reference time," and launching at that time puts apogee in the midnight meridian at summer solstice.

(4a) Schematic view of an orbit launched from Cape Canaveral at the "reference time" (see Fig. 3). The orbit evidently misses the warped plasma sheet, passing on the opposite side of the equator.

(4b) Schematic view for a launch from Kourou (lat. 5^0 N) at the "reference time" of its longitude. Now i_e is (technically) negative and fairly large,

minimizing distant eclipses, but since apogee in mid-summer is placed well north of the ecliptic, plasma coverage is quite good.

(5a) The steady behavior of the semi-major eclipse of a 67-hour orbit over 10 years, after perturbations due to the Moon, Sun and the equatorial bulge of the Earth are taken into account. This is one test for the accuracy of a perturbation code.

(5b) The method used for interpolating positions of the Moon, between two calculated values A and B.

(6) Variation of the perigee height over a 10-year period, for orbits launched July 4, 2000, from initial perigee heights of 1.1, 1.3 and 1.5 Earth radii. Distances are in km. from the center of the Earth. Note the similarities in the semi-annual variation and the long-term trend.

(7) Magnified view of the first 18 months of the lowest trace in Figure 6. Note the semi-monthly variation.

(8a)-(8c) Ten-year variations of orbital parameters of the three orbits in Figure 6: (8a) inclination i to the Earth's equator; (8b) inclination i_e to the plane of the ecliptic; (c) The angle χ between the plane of the ecliptic and the major axis of the orbital ellipse.

Captions to Tables

Table 1a Duration in hours of the longest exclipse, and in parentheses, the number of such eclipses per 12 sample orbits, for 67-hour orbits from Cape Canaveral (apogee near 25 R_E; see text for details). Launches are delayed from -2 to +3 hours from the "reference time," and the angles traversed in the parking orbit before the last stage is fired are given in degrees, from 50^0 to 140^0.

Table 1b Similar to table (1-a), but tabulating the hours spent within 1 R_E of the middle of the (warped) plasma sheet. A score of 1000 approximately equals 1% of the observing time.

Table 2a Similar to table (1-a), but for a 47-hour orbit, apogee near 20 R_E. Eclipses are shorter due to the lower apogee.

Table 2b Similar to table (1-b) but for a 47-hour orbit.

Table 3 Comparison of plasma sheet coverage and eclipse statistics for 15 selected orbits--2 from Cape Canaveral, 7 from Kourou and 6 from intermediate latitudes.

Table 4 Comparison of the coverage of magnetospheric regions by orbits 1-4 of Table 3. The table shows a wide variation in the coverage of the plasma sheet and tail lobes, but hardly any for other regions.

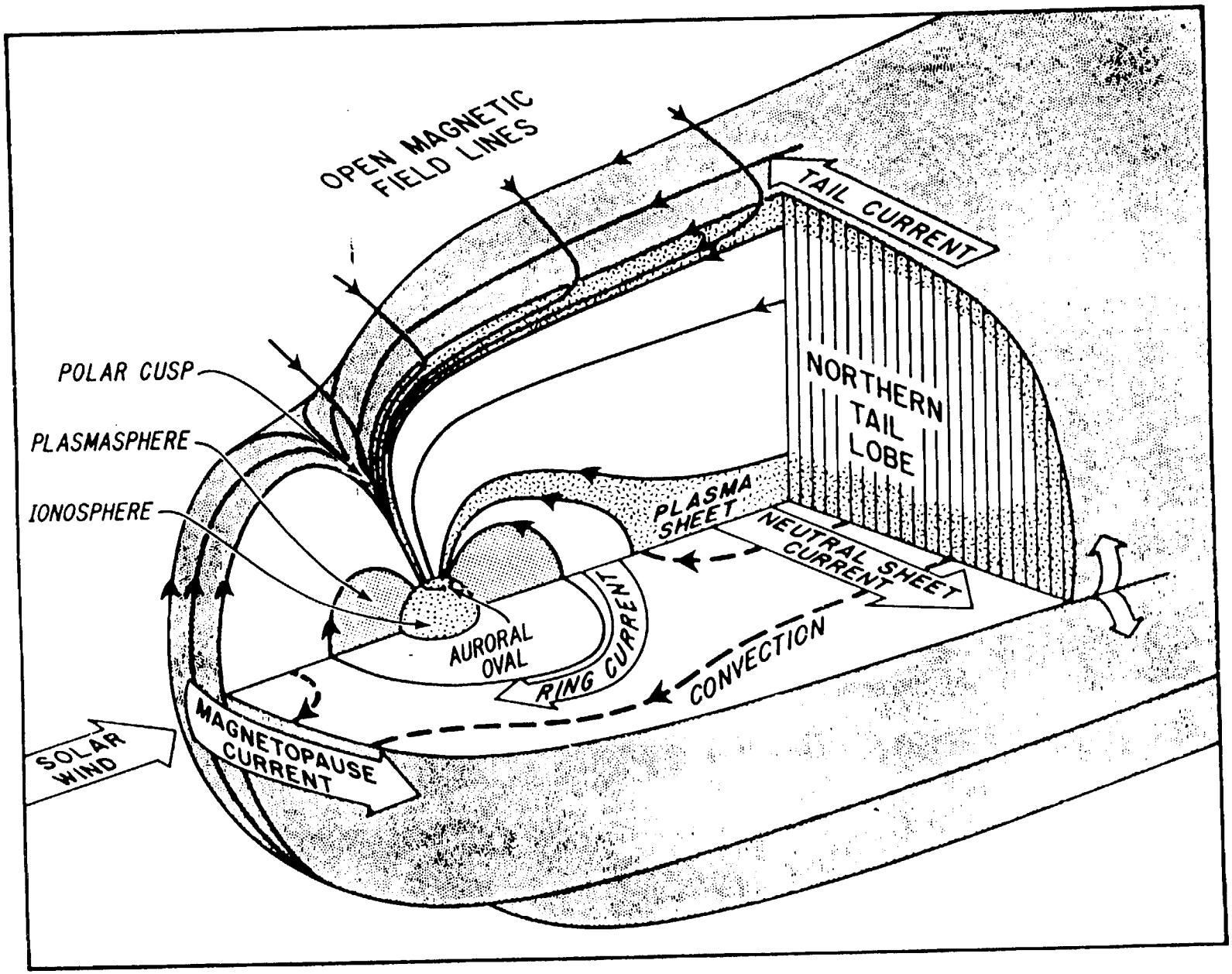
OPEN MAGNETIC FIELD LINES
TAIL CURRENT
POLAR CUSP
PLASMASPHERE
IONOSPHERE
NORTHERN TAIL LOBE
PLASMA SHEET
NEUTRAL SHEET CURRENT
AURORAL OVAL
RING CURRENT
CONVECTION
MAGNETOPAUSE CURRENT
SOLAR WIND

Fig 1

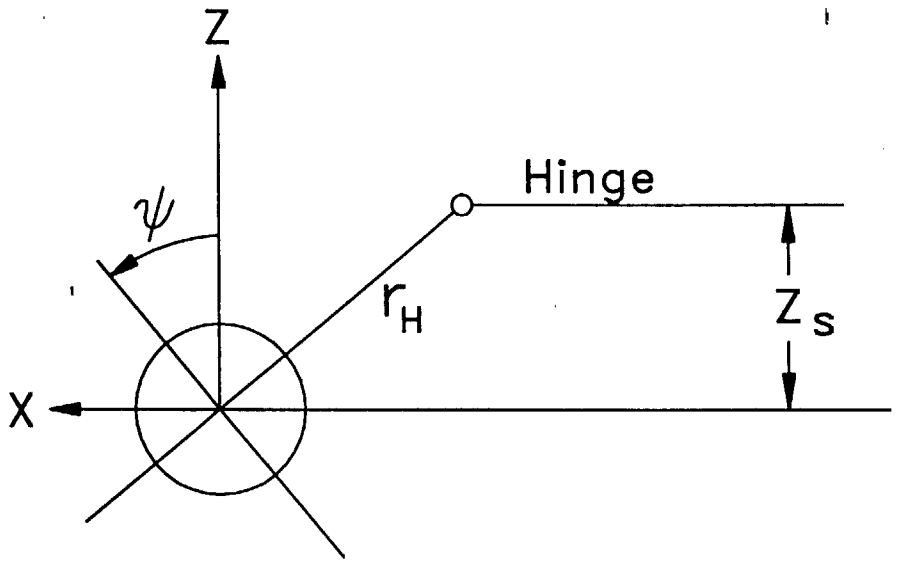

Fig 2a

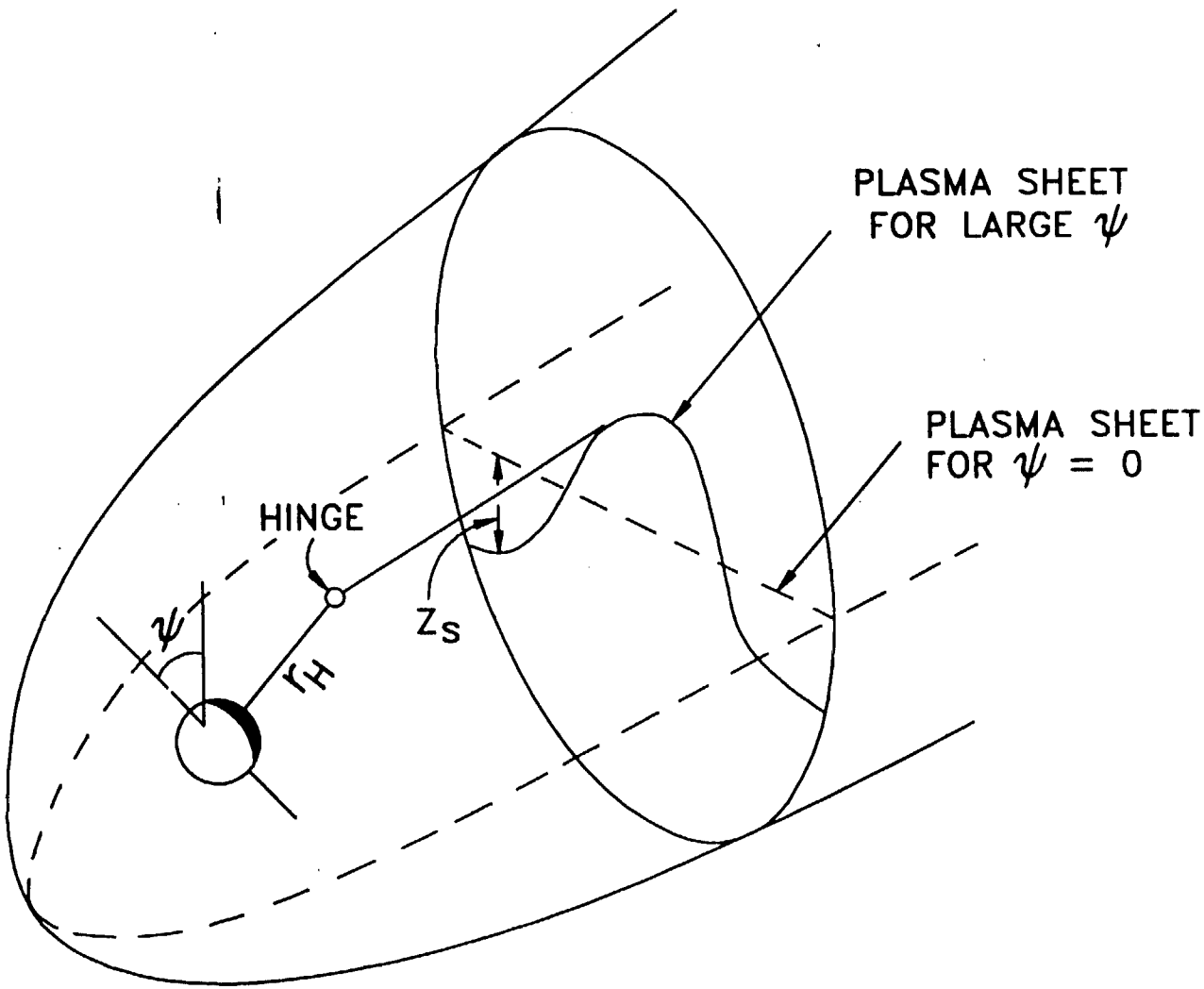
PLASMA SHEET
FOR LARGE ψ
PLASMA SHEET
FOR $\psi = 0$
HINGE
ψ
r_H
Z_S

Fig 2b

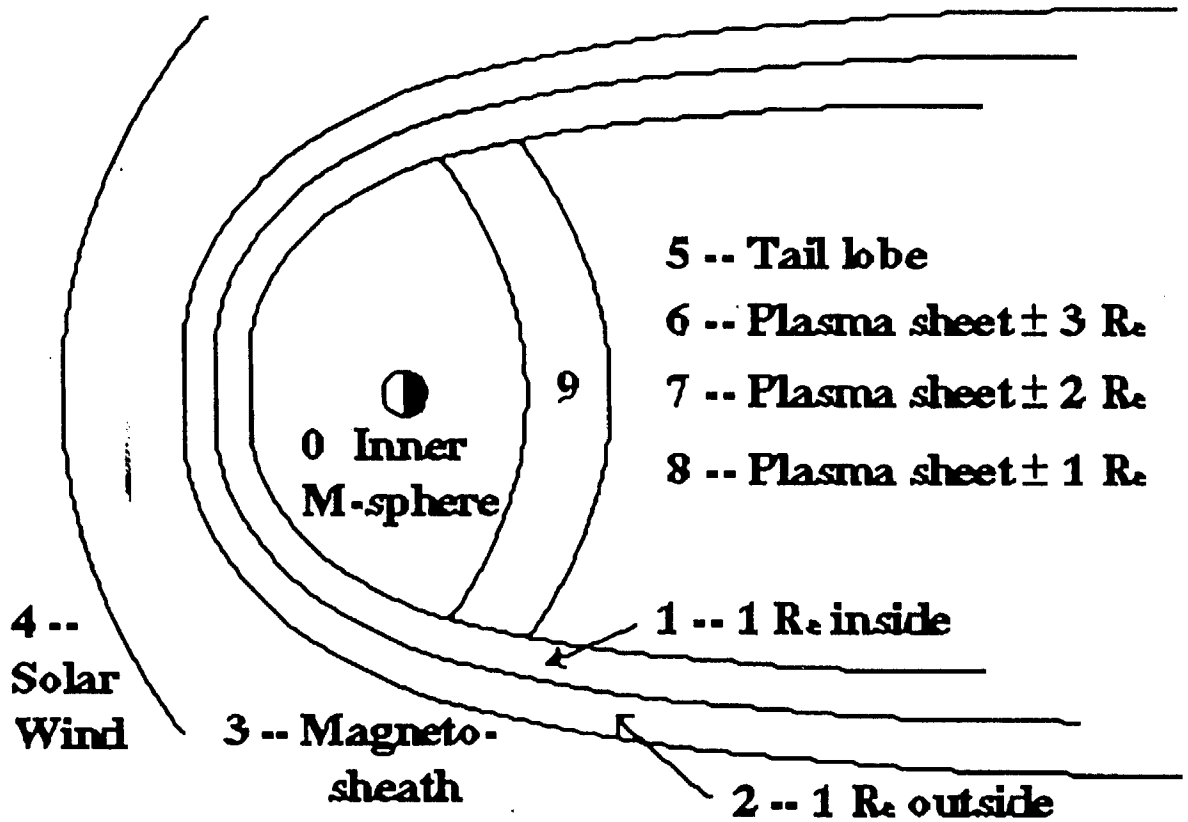
5 -- Tail lobe
6 -- Plasma sheet ± 3 Re
7 -- Plasma sheet ± 2 Re
8 -- Plasma sheet ± 1 Re
9
0 Inner M-sphere
1 -- 1 Re inside
4 -- Solar Wind
3 -- Magneto-sheath
2 -- 1 Re outside

Fig 2c

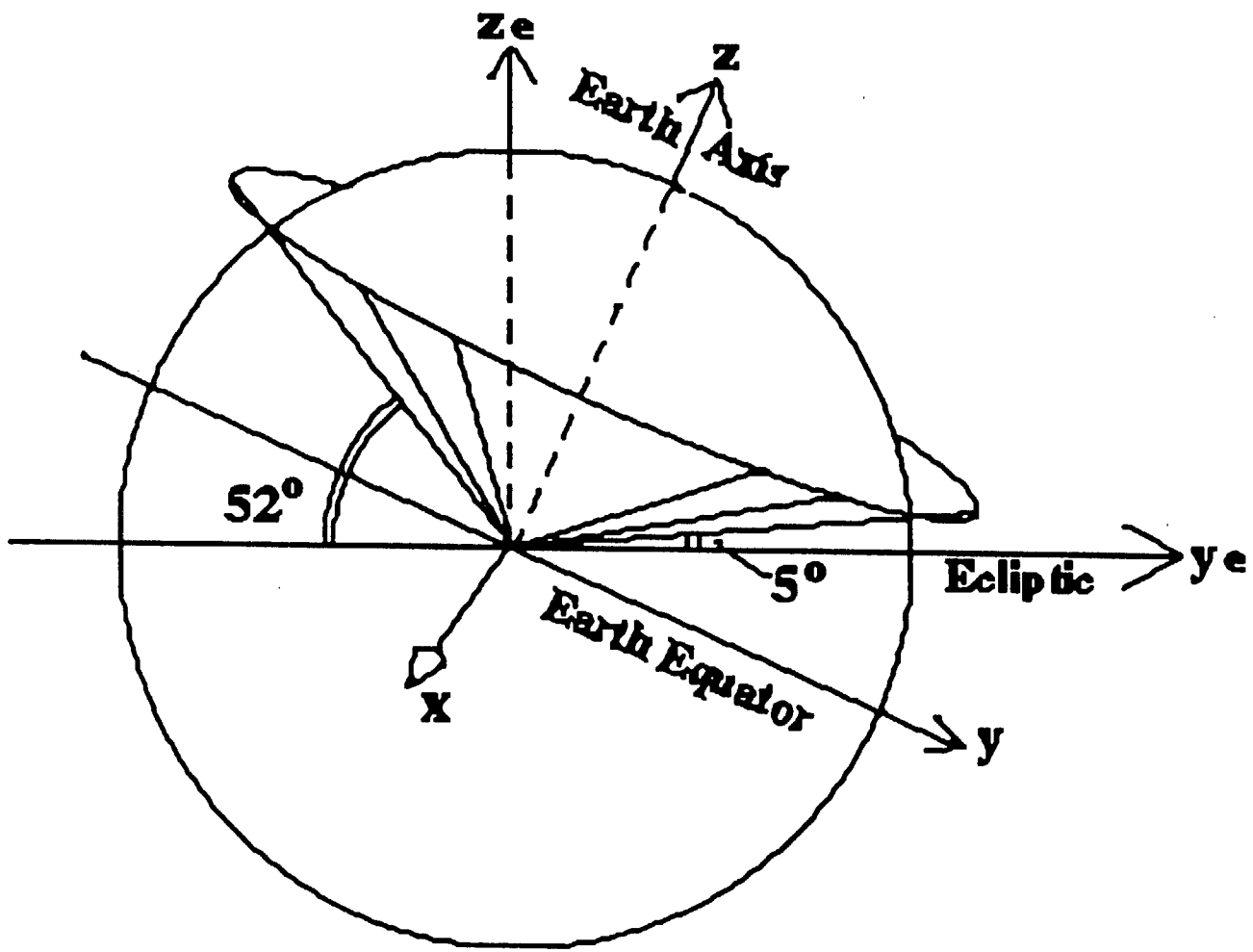

Fig 3

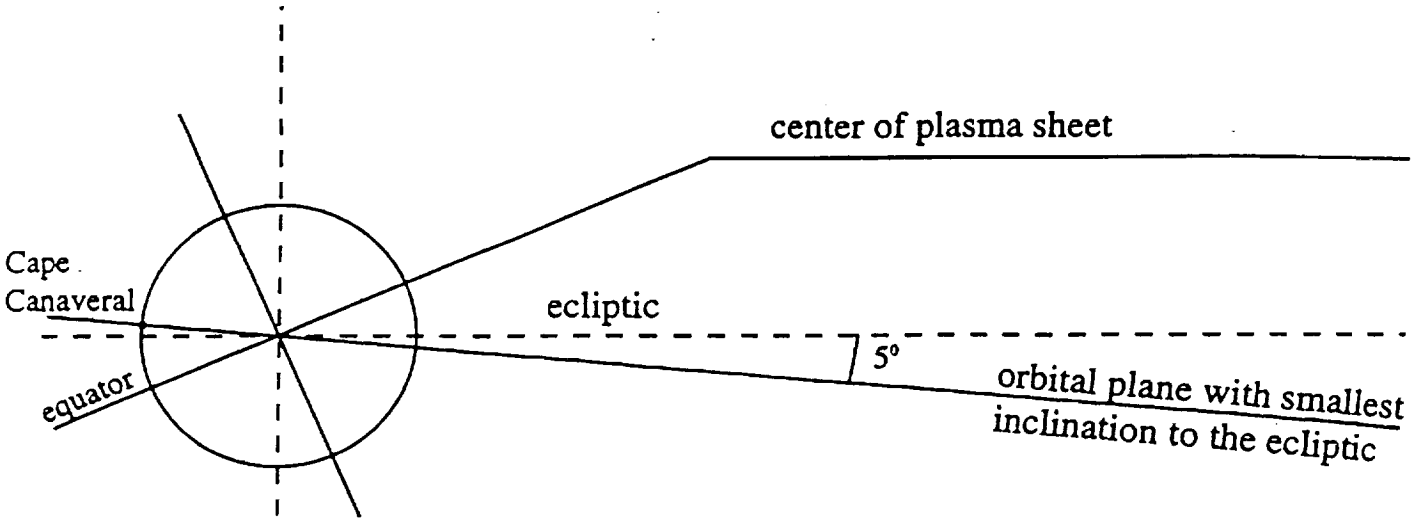

Launch from Cape Canaveral

Fig 4a

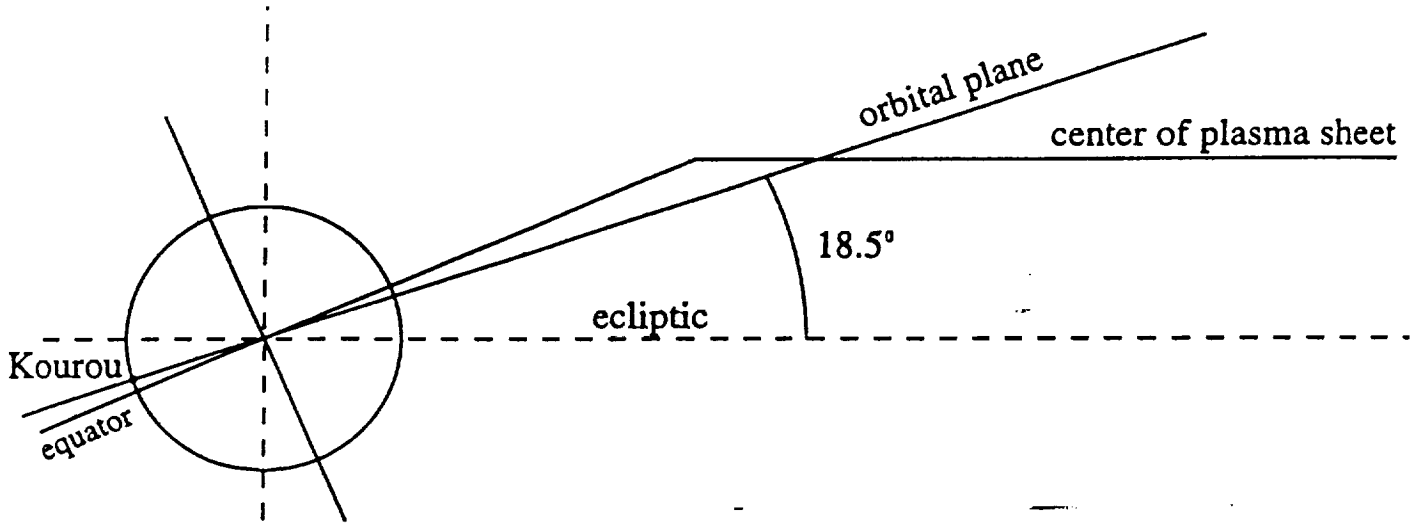

Launch from Kourou
(Latitude 10^0 may be even better)

Fig 4b

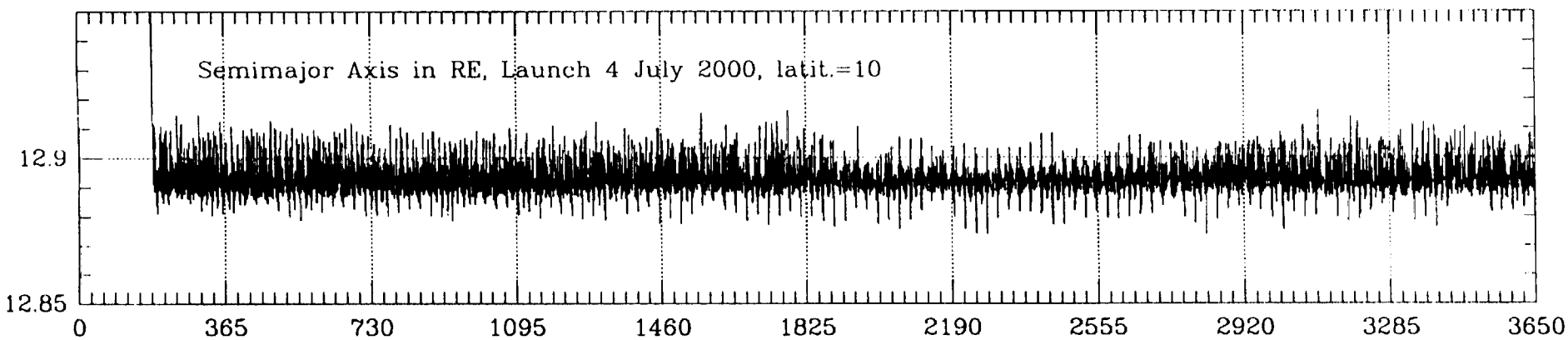
Semimajor Axis in RE, Launch 4 July 2000, latit.=10
12.9
12.85
0
365
730
1095
1460
1825
2190
2555
2920
3285
3650

Fig 5a

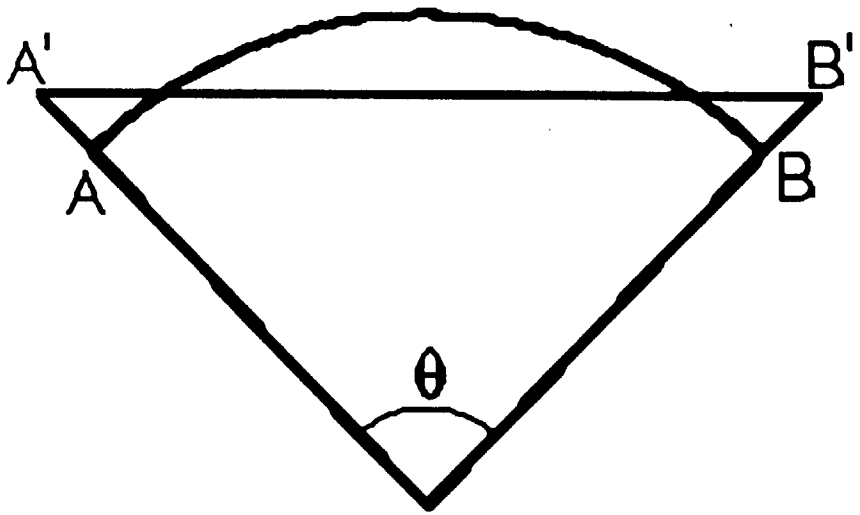

Fig 5b-

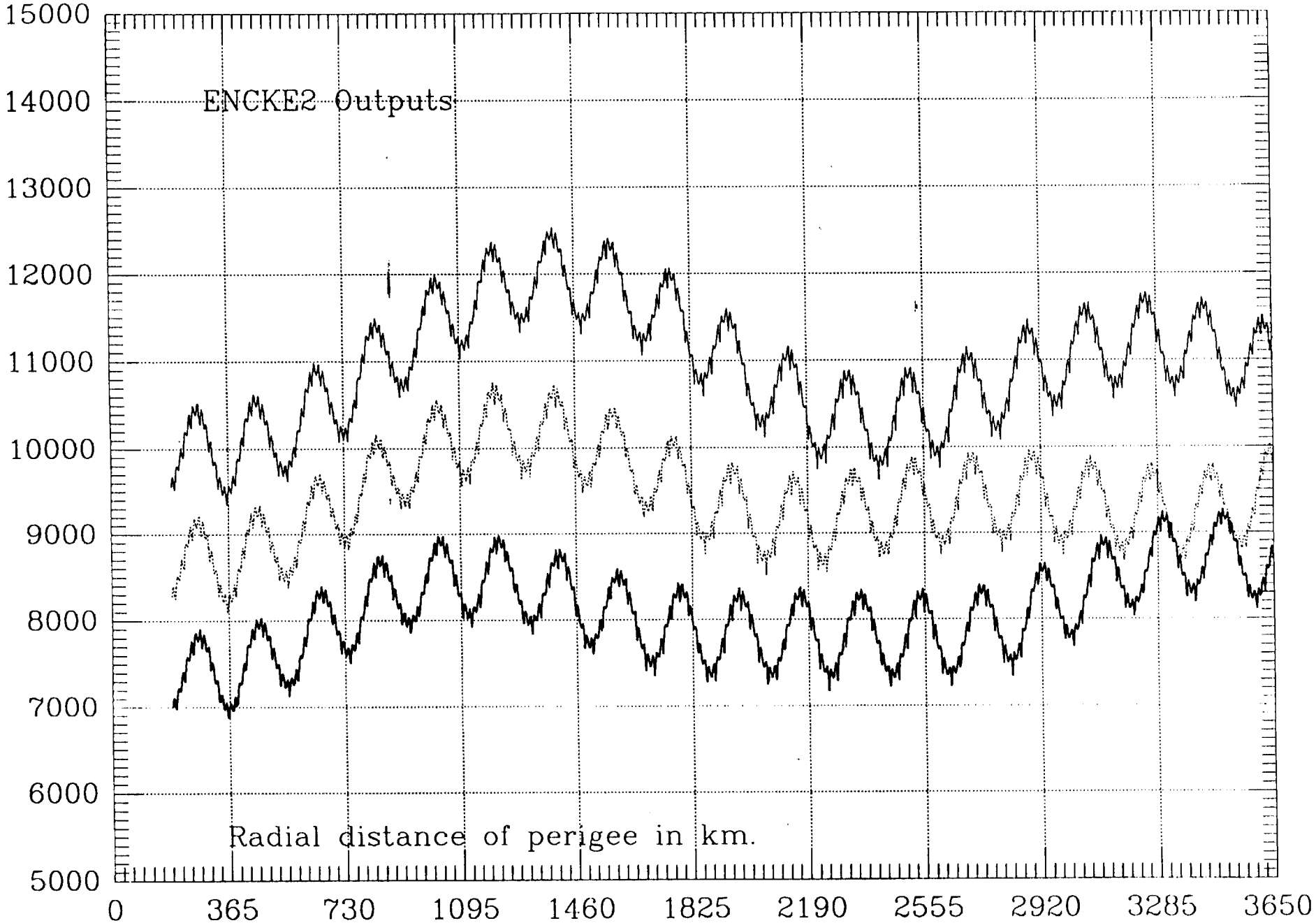
ENCKE2 Outputs
15000
14000
13000
12000
11000
10000
9000
8000
7000
6000
5000
Radial distance of perigee in km.
0
365
730
1095
1460
1825
2190
2555
2920
3285
3650

Fig 6

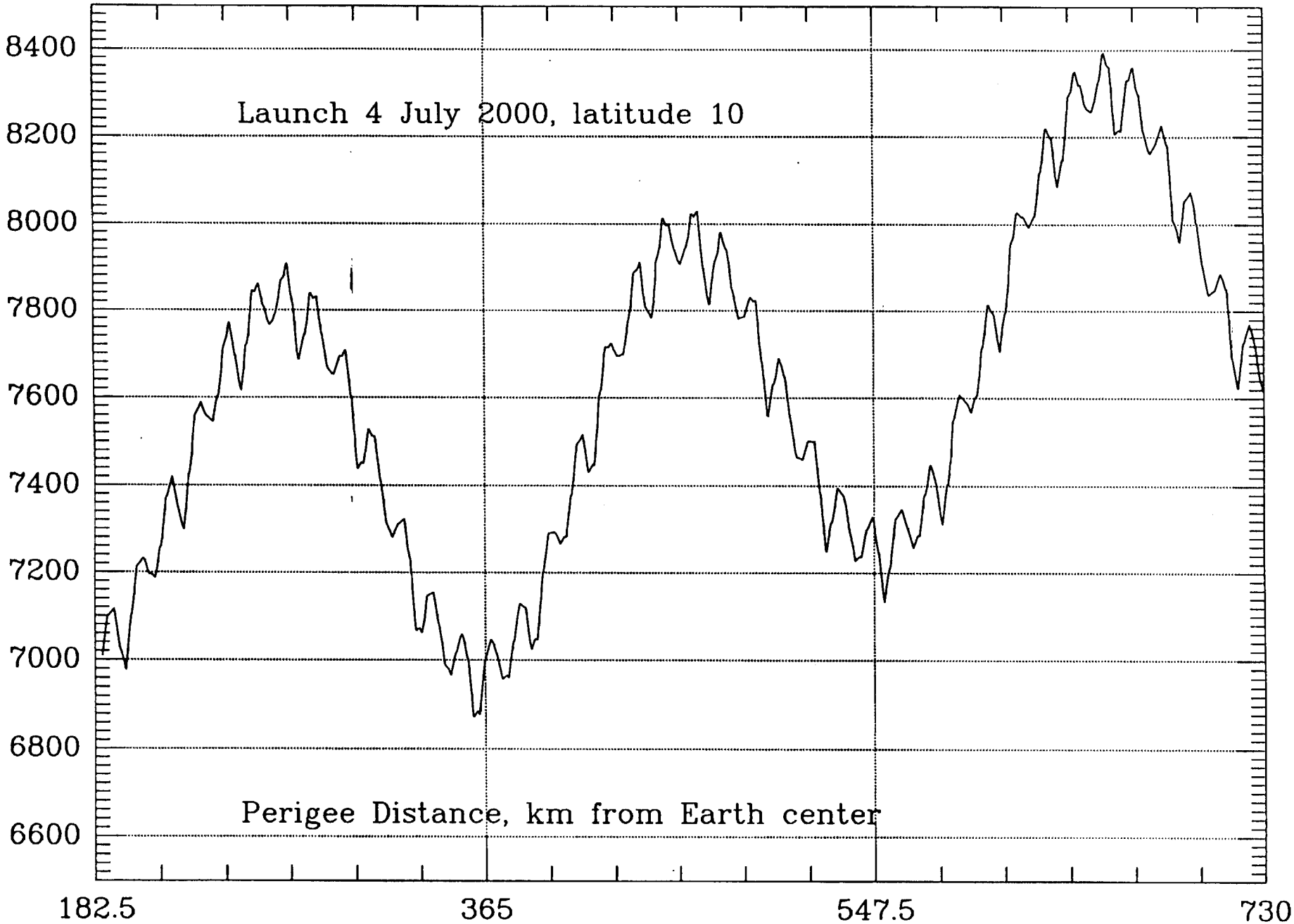
Launch 4 July 2000, latitude 10
Perigee Distance, km from Earth center
8400
8200
8000
7800
7600
7400
7200
7000
6800
6600
182.5
365
547.5
730

Fig 7

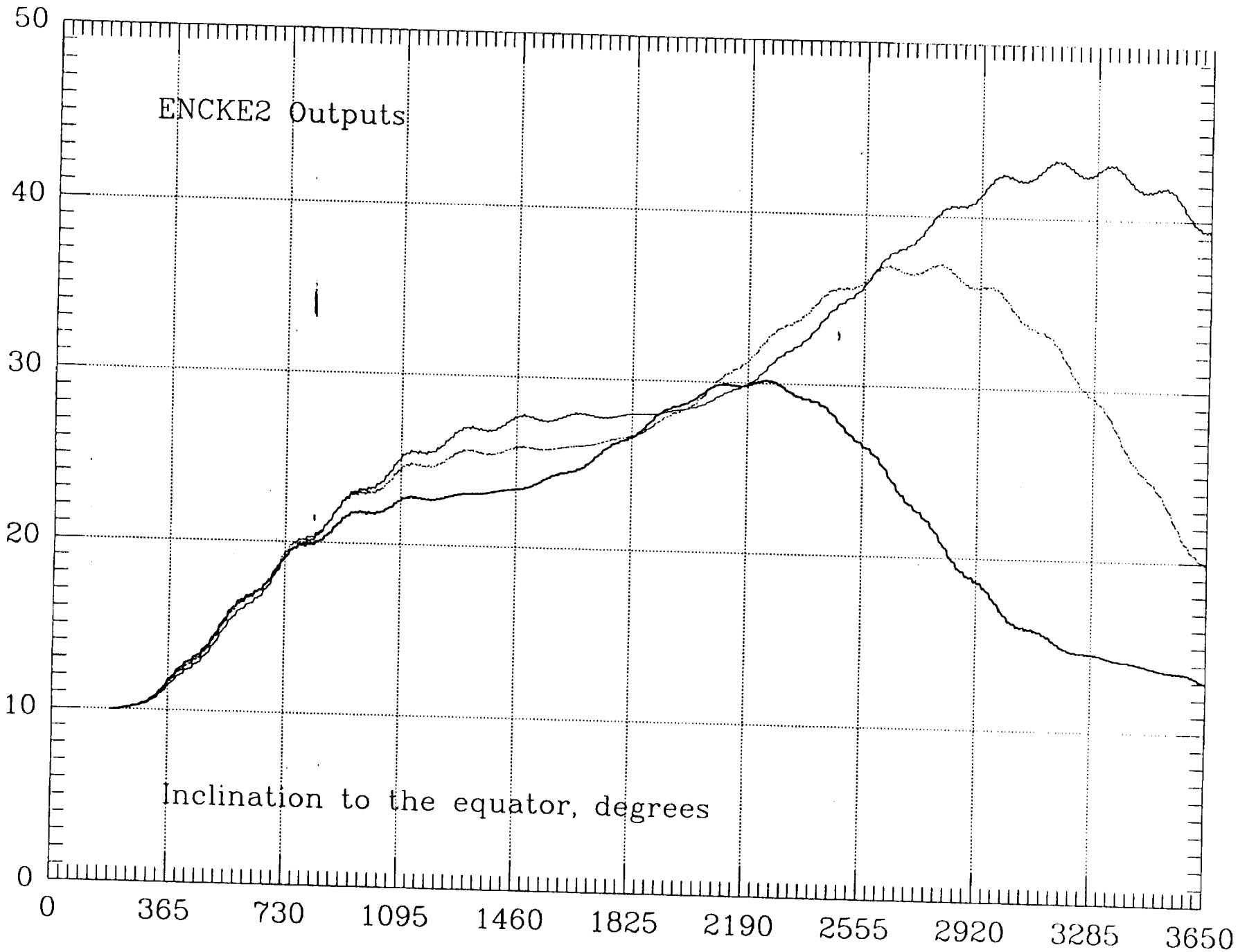
ENCKE2 Outputs
Inclination to the equator, degrees
50
40
30
20
10
0
0
365
730
1095
1460
1825
2190
2555
2920
3285
3650

Fig 8a

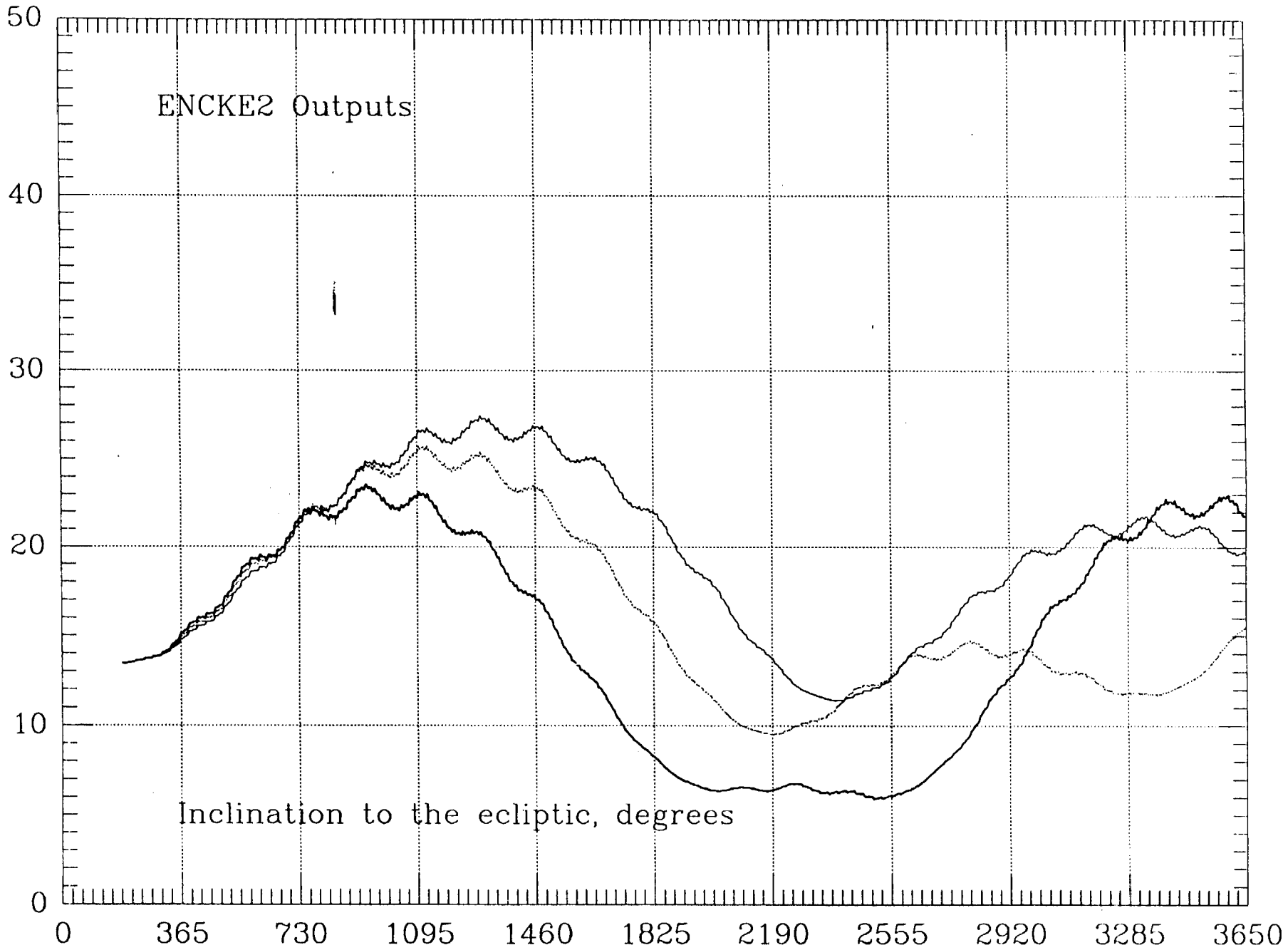
ENCKE2 Outputs
Inclination to the ecliptic, degrees
50
40
30
20
10
0
0
365
730
1095
1460
1825
2190
2555
2920
3285
3650

Fig 8b

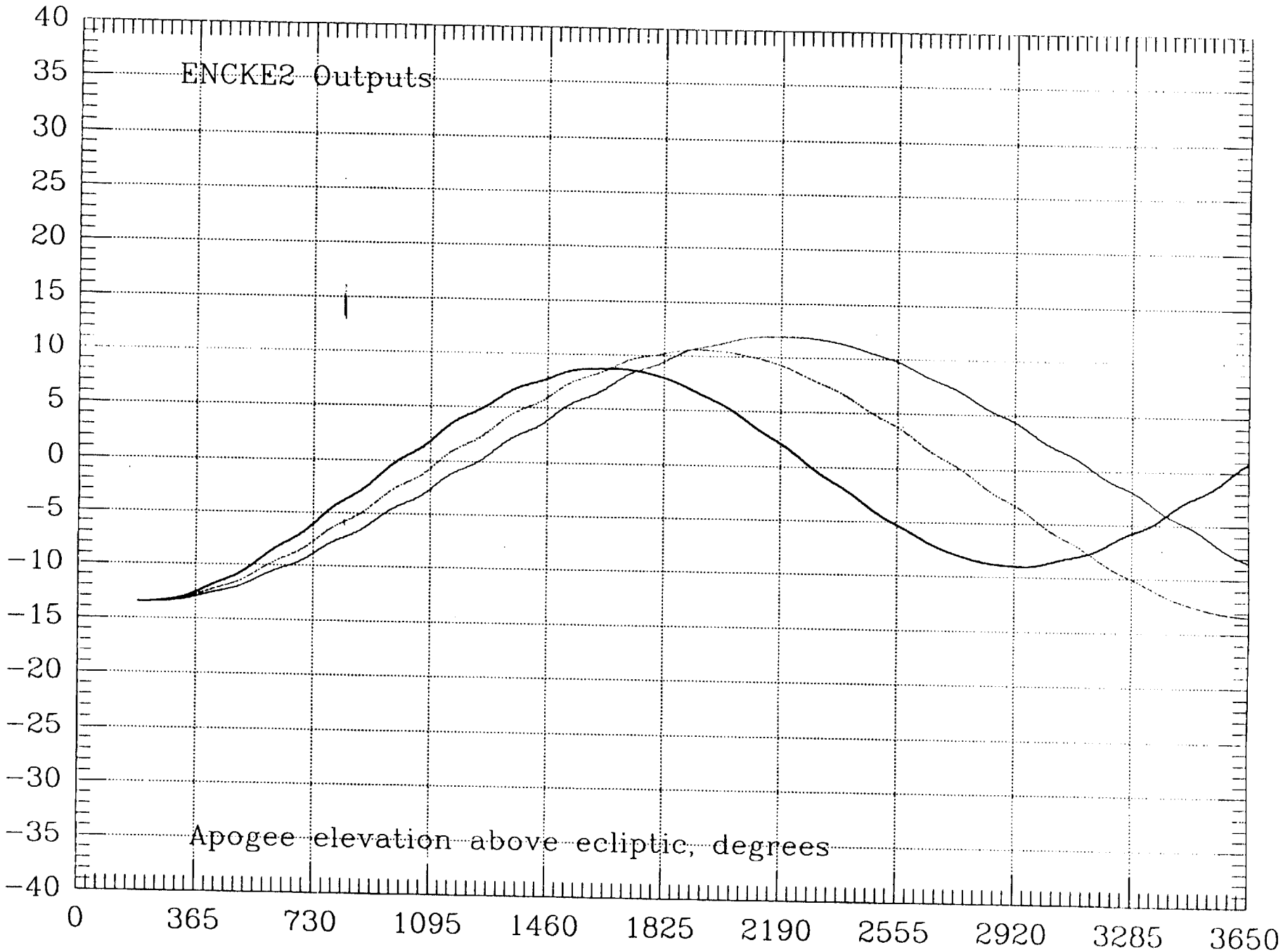
ENCKE2 Outputs
40
35
30
25
20
15
10
5
0
-5
-10
-15
-20
-25
-30
-35
-40
0
365
730
1095
1460
1825
2190
2555
2920
3285
3650
Apogee elevation above ecliptic, degrees

Fig 8c